NJC

PAPER

View Article Online
View Journal | View Issue

Cite this: *New J. Chem.*, 2014, **38**, 5582

Electrochemistry and structural properties of new mixed ligand nickel(II) complexes based on thiosemicarbazone†

Şükriye Güveli,[a] Atıf Koca,[b] Namık Özdemir,[c] Tülay Bal-Demirci*[a] and Bahri Ülküseven[a]

Received (in Victoria, Australia) 11th April 2014,
Accepted 1st September 2014

DOI: 10.1039/c4nj00556b

www.rsc.org/njc

Mixed ligand nickel(II) complexes of 5-chloro-2-hydroxybenzophenone-*N*-R-thiosemicarbazone (R: $-CH_3$ (**L_I**), $-CH_2-CH{=}CH_2$ (**L_{II}**)) and triphenylphosphine were synthesized. The structures of the complexes were characterized by elemental analysis, IR, ^1H and ^{31}P NMR spectroscopy, conductivity, electrochemical and magnetic moment measurements, and single-crystal X-ray diffraction technique. The two nickel(II) complexes have a square planar geometry containing O, N, and S atoms of the thiosemicarbazone, and the P atom of triphenylphosphine. The electrochemical behaviors of the thiosemicarbazone ligands and the nickel complexes were studied using cyclic voltammetry and square wave voltammetry. The redox processes of the compounds were significantly influenced by the central metal ions and the nature of the substituents on the thiosemicarbazones, which are the important factors in controlling the redox properties. *In situ* spectroelectrochemical studies were employed to determine the colors and spectra of the electro-generated species of the complexes.

Introduction

Thiosemicarbazones and their metal complexes have been used in medicine,[1–7] analytic processing,[8] device applications related to telecommunications, and optical information processing for many years.[9–11]

Benzophenones, particularly 2-hydroxybenzophenones, are significant compounds because they have a photo protective effect as ultraviolet absorbers (UVA). They are used as photo stabilizers in cosmetic industry, personal care, sunscreen, skin care products; as additives for preventing photo-oxidation in plastics, coatings, paper and adhesive formulations; and in the manufacture of insecticides, agricultural chemicals, hypnotics, antihistamines, and other pharmaceuticals.[12–16]

Benzophenone thiosemicarbazone compounds and their complexes are of considerable interest, and have been widely studied because of their biological activities and structural properties. A lot of compounds containing thiosemicarbazone ligands have been reported, but there are a limited number of electrochemical studies.[17–22]

Herein, we report the synthesis, the crystal structures and electrochemical behavior of new 5-chloro-2-hydroxybenzophenone-*N*-methyl/allyl-thiosemicarbazidato triphenylphosphine nickel(II) complexes, involving benzophenone and phosphine based on thiosemicarbazone (Scheme 1). The ligands and the complexes were characterized by elemental analysis, UV-Vis spectroscopy, IR, and ^1H and ^{31}P NMR spectroscopy. The molecular structures of the complexes were determined by single crystal X-ray diffraction. The electrochemical behavior of the thiosemicarbazone ligands and the nickel complexes were studied by cyclic voltammetry and square wave voltammetry.

Owing to the variable oxidation states of the nickel centre (III, II and I) and redox activity of the ligand, electrochemical studies[17,22,23] of these complexes are valuable for understanding the influence of the ligand environment on the relative stability of the species in solution. In addition to the electrochemical investigation, *in situ* spectroelectrochemical and *in situ* electro colorimetric studies were employed for the first time to determine the spectra and colors of the electro-generated species of the nickel complexes.

Experimental section

General procedure

All chemicals were of reagent grade and used as commercially purchased without further purification. The elemental analyses were determined on a Thermo Finnigan Flash EA 1112 Series

[a] *Department of Chemistry, Engineering Faculty, Istanbul University, 34320, Avcilar, Istanbul, Turkey. E-mail: tulaybal@istanbul.edu.tr*
[b] *Chemical Engineering Department, Engineering Faculty, Marmara University, 34722, Göztepe, Istanbul, Turkey*
[c] *Department of Physics, Faculty of Arts and Sciences, Ondokuz Mayis University, 55139 Samsun, Turkey*

† CCDC 728286 and 776749. For crystallographic data in CIF or other electronic format see DOI: 10.1039/c4nj00556b

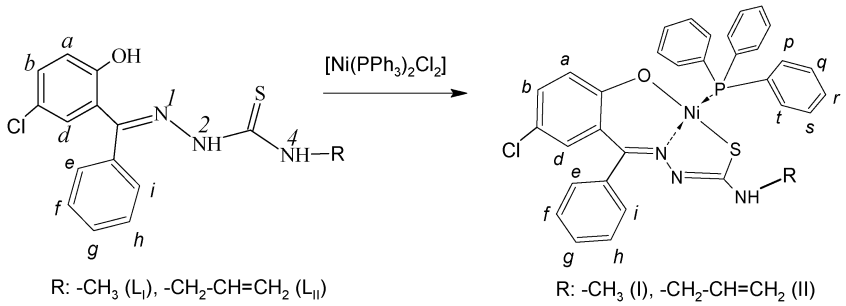

Scheme 1 The formation of the complexes.

Elemental Analyzer and Varian Spectra-220/FS Atomic Absorption spectrometer. The IR spectra of the compounds were recorded on KBr pellets with a Mattson 1000 FT-infrared spectrometer. The ^{1}H- and ^{31}P-Nuclear Magnetic Resonance spectra were recorded on a Bruker AVANCE-500 model spectrometer. The magnetic measurements were carried out at room temperature using the Gouy technique with an MK I model device obtained from Sherwood Scientific. The molar conductivities of the compounds were measured in a 10^{-3} M DMSO solution at 25 ± 1 °C using a digital WPA CMD 750 conductivity meter.

Crystallography

The single-crystal X-ray data of the complexes were collected on a Rigaku RAXIS RAPID diffractometer at 293 K. Graphite-monochromatized Mo Kα radiation (λ = 0.71073 Å) and ω-scan technique were used. The data collection and cell refinement were performed using PROCESS-AUTO[24] software. The data reduction was performed using CrystalStructure[25] program. The structures were solved by direct methods using SHELXS-2013[26] and refined with full-matrix least-squares calculations on F^2 using SHELXL-2014[26] implemented in WinGX.[27] All H atoms were placed geometrically and treated using a riding model, fixing the bond lengths to 0.86, 0.93, 0.97 and 0.96 Å for NH, aromatic CH and terminal CH_2, CH_2 and CH_3 atoms, respectively. The displacement parameters of the H atoms were fixed at U_{iso}(H) = 1.2 U_{eq} (1.5 U_{eq} for methyl) of their parent atoms. Details of the data collection conditions and the parameters of refinement process are given in Table 1. The molecular structure images were generated by using ORTEP-3.[28]

Electrochemistry

Electrochemical and spectroelectrochemical measurements were carried out with a Gamry Reference 600 potentiostat/galvanostat

Table 1 Crystal data and structure refinement parameters for **I** and **II**

Parameter	**I**	**II**
CCDC deposition no.	728286	776749
Color/shape	Dark red/prism	Dark red/prism
Chemical formula	$[Ni(C_{15}H_{12}ClN_3OS)(C_{18}H_{15}P)]$	$[Ni(C_{17}H_{14}ClN_3OS)(C_{18}H_{15}P)]$
Formula weight	638.76	664.80
Temperature (K)	293	293
Wavelength (Å)	0.71073 Mo Kα	0.71073 Mo Kα
Crystal system	Monoclinic	Monoclinic
Space group	$P2_1/a$ (No. 14)	$P2_1/a$ (No. 14)
Unit cell parameters		
a, b, c (Å)	10.9905(3), 22.1006(5), 13.0545(4)	16.6948(3), 10.9984(2), 16.9011(4)
α, β, γ (°)	90, 109.689(2), 90	90, 92.440(2), 90
Volume (Å^3)	2985.51(14)	3100.50(11)
Z	4	4
Calculated density (g cm^{-3})	1.421	1.424
μ (mm^{-1})	0.895	0.865
Absorption correction	Multi-scan	Multi-scan
T_{min}, T_{max}	0.637, 0.914	0.570, 0.917
F_{000}	1320	1376
Crystal size (mm^3)	0.60 × 0.10 × 0.10	0.50 × 0.20 × 0.10
Diffractometer/measurement method	Rigaku RAXIS-RAPID/ω scan	Rigaku RAXIS-RAPID/ω scan
Index ranges	$-12 \le h \le 13$, $-26 \le k \le 26$, $-15 \le l \le 15$	$-20 \le h \le 20$, $-13 \le k \le 13$, $-18 \le l \le 20$
Theta range for data collection (°)	$2.17 \le \theta \le 25.12$	$3.24 \le \theta \le 25.49$
Reflections collected	56201	59264
Independent/observed reflections	5305/5252	5730/5645
R_{int}	0.069	0.059
Refinement method	Full-matrix least-squares on F^2	Full-matrix least-squares on F^2
Data/restraints/parameters	5305/0/370	5730/0/388
Goodness-of-fit on F^2	1.082	1.054
Final R indices [$I > 2\sigma(I)$]	R_1 = 0.0952, wR_2 = 0.2489	R_1 = 0.0402, wR_2 = 0.1180
R indices (all data)	R_1 = 0.0965, wR_2 = 0.2500	R_1 = 0.0410, wR_2 = 0.1191
$\Delta\rho_{max}$, $\Delta\rho_{min}$ (e Å^{-3})	0.71, −0.33	0.88, −0.32

utilizing a three-electrode configuration at 25 °C. For cyclic voltammetry (CV), controlled potential coulometry (CPC), and square wave voltammetry (SWV) measurements, the working electrode was a Pt disc with a surface area of 0.071 cm^2. The surface of the working electrode was polished with a diamond suspension before each run. Pt wire served as the counter electrode. Saturated calomel electrode (SCE) was employed as the reference electrode and separated from the bulk of the solution by a double bridge. Ferrocene was used as an internal reference. Tetrabutylammonium perchlorate (TBAP) in dimethylsulfoxide (DMSO) or acetonitrile (MeCN) was employed as the supporting electrolyte at a concentration of 0.10 mol dm^{-3}. High purity N_2 was used to remove dissolved O_2 at least 15 minutes prior to each run and to maintain a nitrogen blanket during the measurements. IR compensation was applied to the CV and SWV scans to minimize the potential control error.

UV/Vis absorption spectra and chromaticity diagrams were measured using an Ocean Optics QE65000 diode array spectrophotometer. *In situ* spectroelectrochemical and *in situ* electrocolorimetric measurements were carried out using a three-electrode configuration of thin-layer quartz spectroelectrochemical cell at 25 °C. The working electrode was a Pt tulle. A Pt wire counter electrode and a SCE reference electrode separated from the bulk of the solution by a double bridge were used. The standard illuminant A with a 2 degree observer at a constant temperature in a light booth designed to exclude external light was used. Prior to each set of measurements, the background color coordinates (*x*, *y* and *z* values) were taken at the open-circuit using the electrolyte solution without complexes under study. During the measurements, readings were taken as a function of time under kinetic control.

Synthesis of 5-chloro-2-hydroxybenzophenone-*N*-methyl/allyl-thiosemicarbazone

5-Chloro-2-hydroxybenzophenone-*N*-methyl-thiosemicarbazone (**L_I**) and 5-chloro-2-hydroxybenzophenone-*N*-allyl-thiosemicarbazone (**L_{II}**) ligands were synthesized by reactions of 5-chloro-2-hydroxybenzophenone with *N*-methyl-thiosemicarbazide or *N*-allyl-thiosemicarbazide according to the procedure described in the literature.[29] The colors, yields (%), m.p. (°C), elemental analysis, UV-Vis [$\lambda_{max}(\log \varepsilon)$], IR (KBr, cm^{-1}) and ^{1}H NMR (ppm, *J* in Hz) data of the ligands are as follows:

L_I. Cream, 80%, 94–95, anal. calc. For $C_{15}H_{14}ClN_3OS$ (319.81 g): C, 56.33; H, 4.41; N, 13.14; S, 10.03. Found: C, 56, 36; H, 4.40; N, 13.17; S, 9.99%. UV-Vis: 237 (4.52), 317 (4.33), 330 (shoulder 4.45). IR (KBr, cm^{-1}): ν(OH) 3325, $\nu(N^4H)$ 3369, $\nu(N^2H)$ 3285, $\delta(N^4H)$ 1646, (N^2H) 1624, ν(C═N) 1605, ν(–CS–NH) 1556, ν(C═S) 1274, ν(C–O) 1240. ^{1}H-NMR (500 MHz, $CDCl_3$, ppm): 11.82, 10.50 (*cis*/*trans* ratio, 1/2, s, 1H, O*H*), 8.49, 8.39 (*cis*/*trans* ratio, 3/2, s, 1H, N^2H), 7.62 (dd, *J* = 1.46, *J* = 8.29, 1H, *d*), 7.58–7.46 (m, 3H, *f, g, h*), 7.40–7.22 (m, 2H, *e, i*), 7.01 (d, *J* = 2.93, 1H, *b*), 6.91 (dd, *J* = 4.39, *J* = 8.78, 1H, *a*), 6.75 (br s, 1H, N^4H), 3.21 (d, *J* = 4.88, *J* = 9.27, 3H, N^4–CH_3).

L_{II}. Cream, 75%, 168–169, anal. calc. For $C_{17}H_{16}ClN_3OS$ (345.85 g): C, 59.04; H, 4.66; N, 12.15; S, 9.27. Found: C, 59, 36; H, 4.56; N, 12.17; S, 9.25%. UV-Vis: 241 (4.44), 307 (shoulder 4.68), 315 (4.46), 347 (4.48). IR (KBr, cm^{-1}): ν(OH) 3237, $\nu(N^4H)$ 3466, $\nu(N^2H)$ 3214, $\delta(N^4H)$ 1647, (N^2H) 1612, ν(C═N) 1593, ν(–CS–NH) 1556, 1285, ν(C═S) 1227, ν(C–O) 1231. ^{1}H-NMR (500 MHz, DMSO-d_6, ppm): 10.52 (s, 1H, O*H*), 8.40 (s, 1H, N^2H), 7.60 (t, *J* = 1.46, *J* = 8.29, *d*), 7.58–7.55 (m, 2H, *f, h*), 7.49–7.47 (m, 1H, *g*), 7.18 (dd, *J* = 2.44, *J* = 8.78, 2H, *e, i*), 6.91 (d, *J* = 8.78, 1H, *b*), 6.77 (br s, 1H, N^4H), 6.64 (d, *J* = 2.45, 1H, *a*), 5.93–5.87 (m, 1H, –*CH*═), 5.23 (d, *J* = 17.08, 1H, ═CH_{2a}), 5.18 (d, *J* = 10.25, 1H, ═CH_{2b}), 4.30 (s, 1H, N^4–CH_2).

Synthesis of the complexes

5-Chloro-2-hydroxybenzophenone-*N*-methylthiosemicarbazidato triphenylphosphine–nickel(II) complex (**I**) was synthesized by the reaction of 5-chloro-2-hydroxybenzophenone-*N*-methyl thiosemicarbazone (**L_I**) and $[Ni(PPh_3)_2Cl_2]$ using the literature method (in Scheme 1).[30,31] The color, yield (%), m.p. (°C), μ_{eff} (BM), molar conductivity (in 10^{-3} M DMSO, ohm^{-1} cm^2 mol^{-1}), calculated (found) analytical, UV-Vis [$\lambda_{max}(\log \varepsilon)$], FT-IR (KBr, cm^{-1}), ^{1}H NMR (500 MHz, ppm, *J* in Hz), and ^{31}P NMR data of the complexes are given as follows.

I. Dark red, 88%, 250–252, 0.1, 4.9, anal. calc. For $C_{33}H_{27}ClN_3NiOPS$ (638.77 g): C, 62.05; H, 4.26; N, 6.58; S, 5.02; Ni, 9.19. Found: C, 62.09; H, 4.27; N, 6.49; S, 5.00; Ni, 9.01%. UV-Vis: 241 (4.26), 249 (sh. 4.25), 280 (sh. 4.09), 343 (sh. 3.76), 352 (3.77), 371 (3.76), 379 (sh, 3.74), 418 (3.47), 439 (3.26). IR (KBr, cm^{-1}): $\nu(N^4H)$ 3428, ν(C═CH_2) 3096, 3052, 3030, ν(–CH_2–) 2920, 2856, $\delta(N^4H)$ 1632, ν(C═N^1) 1559, ν(C═N^2) 1532, ν(C–O) 1248, $\nu(PPh_3)$ 1438, 1098, 1030, 1003, 742, 696, ν(–C–S) 881. ^{1}H-NMR (500 MHz, DMSO-d_6, ppm): 7.75–7.69 (m, 6H, *p, t*), 7.44–7.41 (m, 3H, r), 7.37–7.33 (m, 8H, *f, h, q, s*), 7.28 (t, *J* = 7.32, 1H, *g*), 7.13 (d, *J* = 8.29, 2H, *e, i*), 6.80 (dd, *J* = 2.44, *J* = 8.79, 1H, *d*), 6.66 (d, *J* = 2.44, 1H, *a*), 6.64 (d, *J* = 9.27, 1H, *b*), 4.30 (br s, 1H, N^4H), 2.20 (s, 3H, N^4–CH_3). ^{31}P NMR: 19.56.

II. Dark red, 80%, 212–214, 0.05, 3.8, anal. calc. For $C_{35}H_{29}ClN_3NiOPS$ (664.81 g): C, 63.23; H, 4.40; N, 6.32; S, 4.82; Ni, 8.83. Found: C, 63.19; H, 4.45; N, 6.42; S, 4.78; Ni, 9.22%. UV-Vis: 244 (4.66), 284 (sh. 4.44), 314 (sh. 4.19), 376 (4.15), 419 (3.92), 440 (3.60). IR (KBr, cm^{-1}): $\nu(N^4H)$ 3406, ν(C═CH_2) 3061, 3051, 3007, ν(–CH_2–) 2920, 2854, $\delta(N^4H)$ 1632, ν(C═N^1) 1587, ν(C═N^2) 1554, ν(C–O) 1242, $\nu(PPh_3)$ 1435, 1095, 1030, 997, 746, 696, ν(–C–S) 873. ^{1}H-NMR (500 MHz, DMSO-d_6, ppm): 7.77–7.73 (m, 6H, *p, t*), 7.44–7.41 (m, 3H, r), 7.37–7.34 (m, 8H, *f, h, q, s*), 7.28 (t, *J* = 7.32, 1H, *g*), 7.11 (d, *J* = 6.84, 2H, *e, i*), 6.81 (dd, *J* = 2.44, *J* = 8.78, 1H, *d*), 6.66 (d, *J* = 2.93, 1H, *a*), 6.20 (d, *J* = 8.79, 1H, *b*), 4.41 (s, 1H, N^4H), 3.24 (s, 2H, N^4–C*H*), 5.57–5.49 (m, 1H, –C*H*═), 4.85 (d, *J* = 10.25, *J* = 13.67, 2H, ═CH_2), 4.84 (d, *J* = 10.25, 1H, ═CH_{2b}), 5.18 (d, *J* = 17.08, 1H, ═CH_{2a}), 4.30 (s, 1H, N^4–CH_2). ^{31}P NMR: 21.35.

Results and discussion

Synthesis and spectral studies

Reactions of the ligands (**L_I**, **L_{II}**) with $[Ni(PPh_3)_2Cl_2]$ yielded stable complexes (**I**, **II**) with the general formula, $[Ni(L)PPh_3]$. The complexes behaving as a non-electrolyte were red crystals

and dissolved in common organic solvents. The μ_{eff} values showed that the complexes are diamagnetic and revealed the square planar geometry of the low-spin nickel ion. Thiosemicarbazone and triphenylphosphine are coordinated to the central nickel ion *via* phenolic O, hydrazine N, thiol S and phosphine P atoms.

The UV spectrum of the ligands showed bands at 237, 317 and 330 nm for $\mathbf{L_I}$ and 241, 307, 315, and 347 nm for $\mathbf{L_{II}}$, which were attributed $\pi \rightarrow \pi^*$ and $n \rightarrow \pi^*$ transitions corresponding to phenol, aromatic and vinyl groups. In the spectrum of the complexes, the bands at 241, 249, 280, 343, and 352 nm for **I**, at 244, 284 and 314 nm for **II** were assigned to transitions in the ligand. The band at 330 nm and 347 nm in the ligand spectrum for $\mathbf{L_I}$ and $\mathbf{L_{II}}$, respectively, shifted to 352 and 376 nm, which was assigned to the thioamide $n \rightarrow \pi^*$ transition of the complexation of thiolate sulphur. The medium-intensity bands at 418 and 439 for **I** and at 419 and 440 nm for **II** are due to metal–ligand charge transfer processes.[32] The bands assigned to d–d, Laporte forbidden, spin-allowed transitions of the Ni(II) ion were not recorded because of its low intensity.

The stretching and intraplanar bending bands assigned to $\nu(OH)_{phenol}$ and $\delta(N^2H)$ in the ligands, at 3325 and 3237 cm^{-1} and at 1624 and 1612 cm^{-1}, were absent in the IR spectra of the complexes. This confirms the thio-enol tautomerism of ligand in the complexes; *i.e.*, the thiol group and hydroxyl group *via* deprotonation are connected to the metal centre. The stretching bands $\nu(C{=}N^1)$ observed at 1605 cm^{-1} (for $\mathbf{L_I}$) and 1593 cm^{-1} (for $\mathbf{L_{II}}$) shifted to 1587 cm^{-1} (for **I**) and 1554 cm^{-1} (for **II**) on complexation. This shift indicates the coordination of thiosemicarbazone through azomethine nitrogen atoms to the metal centre. Furthermore, the new bands at 1559 cm^{-1} (for **I**) and 1532 cm^{-1} (for **II**) in the complexes were assigned to $\nu(C{=}N^2)$ vibrations of the newly formed CN group.

The signals observed at δ *ca.* 11.16 ppm (for $\mathbf{L_I}$) and 10.52 ppm (for $\mathbf{L_{II}}$) in the free ligands disappear in the complexes. This suggests that phenolic oxygen atom coordinates to the metal atom *via* deprotonation. The $\delta(N^2H)$ proton signals, which appear at δ *ca.* 8.44 (for $\mathbf{L_I}$) and 8.40 (for $\mathbf{L_{II}}$) ppm in the ^1H NMR spectra of the thiosemicarbazone ligands, disappear in the complexes. The disappearance of the N^2H proton signals indicates the collapse of the thioamide structure of the thiosemicarbazone and its coordination to the metal centre through thiol sulphur atoms in the enol form. The amine proton signals (N^4H) observed at δ 6.75 ($\mathbf{L_I}$) and 6.77 ($\mathbf{L_{II}}$) ppm in the thiosemicarbazones emerge at δ 4.30 (for **I**) and 4.41 (for **II**) ppm in the complexes. The (N^4H) signals were monitored upfield because of intramolecular interactions in the spectra of the thiosemicarbazone ligands. The phenyl protons of thiosemicarbazone and triphenylphosphine appeared in the δ 7.77–6.20 ppm region in all the complexes.

In the ^{31}P NMR spectra of the complexes, the bands observed in the range of 19.56–21.35 ppm were attributed to the P atom in the basal plane.[31]

Structural description of the complexes

The solid-state structures of **I** and **II** were verified by single-crystal X-ray analysis. The ORTEP-3 views of the complexes with the atomic numbering scheme are depicted in Fig. 1 and 2, respectively,

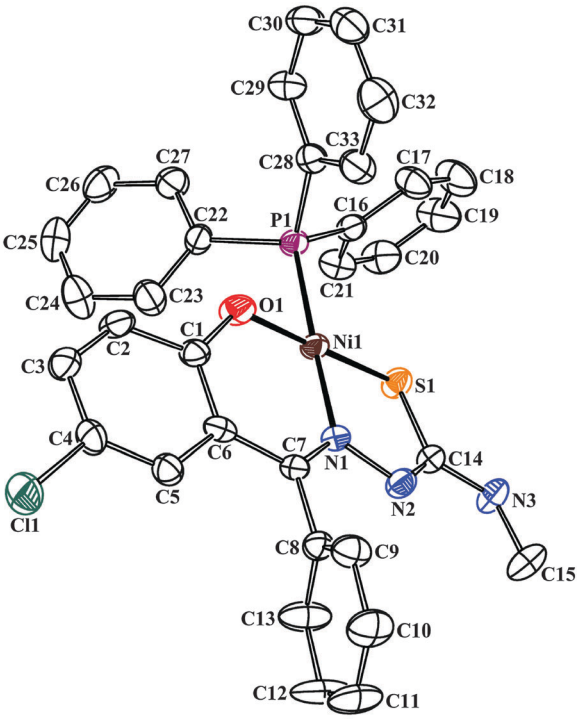

Fig. 1 A view of **I** showing the atom-numbering scheme. The displacement ellipsoids are drawn at the 30% probability level. Hydrogen atoms have been omitted for the sake of clarity.

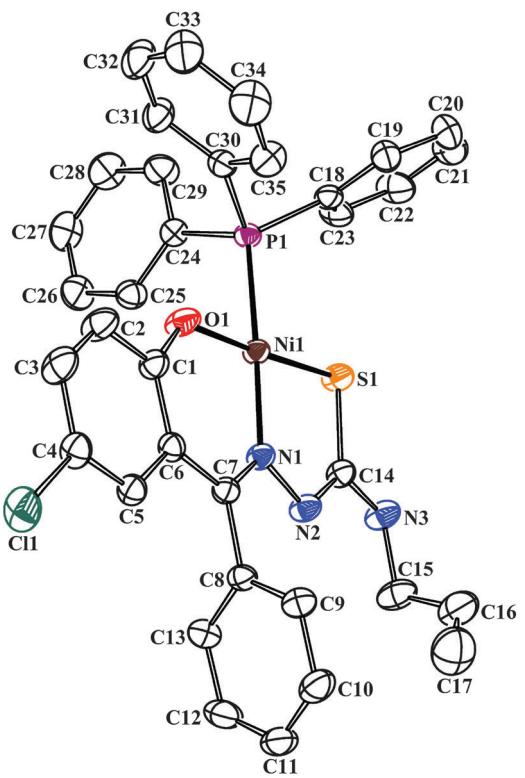

Fig. 2 A view of **II** showing the atom-numbering scheme. The displacement ellipsoids are drawn at the 30% probability level. Hydrogen atoms have been omitted for the sake of clarity.

Table 2 Selected geometrical parameters for **I** and **II**

Parameter	I	II
Bond lengths (Å)		
Ni1–S1	2.128(2)	2.1262(7)
Ni1–P1	2.1824(19)	2.1994(6)
Ni1–O1	1.831(5)	1.8342(18)
Ni1–N1	1.896(5)	1.8897(19)
Bond angles (°)		
O1–Ni1–N1	95.0(2)	94.88(8)
O1–Ni1–S1	176.38(18)	176.71(6)
N1–Ni1–S1	88.25(18)	88.39(6)
O1–Ni1–P1	84.83(16)	86.97(6)
N1–Ni1–P1	177.92(19)	175.49(7)
S1–Ni1–P1	91.99(8)	89.78(2)
Torsion angles (°)		
C1–C6–C7–N1	−8.2 (11)	−0.1 (4)
N1–C7–C8–C9	109.0(9)	99.2(3)
C6–C7–N1–N2	−178.0(6)	−178.2(2)
C7–N1–N2–C14	171.0(6)	−175.6(2)
N3–C14–N2–N1	−179.8(6)	−178.4(2)
N2–C14–N3–C15	1.2(12)	−7.0(4)
S1–C14–N3–C15	−178.8(7)	172.7(2)
N3–C15–C16–C17	—	126.3(5)

while selected geometric parameters are given in Table 2. The complexes contain a thiosemicarbazone ligand with a Ni^{II} metal centre and one triphenylphosphine ligand. The difference in the composition of the two complexes originates from the tridentate thiosemicarbazone ligand. However, the crystallization characteristics of the complexes are the same with both crystallizing in monoclinic space group $P2_1/a$.

The thiosemicarbazone ligands become doubly deprotonated to act as O, N and S tridentate ligands by coordinating *via* its phenolate oxygen, O1, azomethine nitrogen, N1, and thiolato sulfur atom, S1, in the deprotonated form after thiol formation, giving a square planar geometry around the nickel atoms. The triphenylphosphine ligands coordinate in the fourth position. In the square-planar coordination, atoms Ni1, S1, P1, O1 and N1 deviate by −0.0028(16), −0.0293(18), 0.0317(18), −0.0344(21) and 0.0348(19) Å for **I**, −0.0262(7), −0.0318(8), 0.0439(8), −0.0352(9) and 0.0492(9) Å for **II**, respectively, from the mean plane through these five atoms. The five- and six-membered chelate rings formed upon coordination are not coplanar with a dihedral angle of 11.01(12)° for **I** and 4.64(10)° for **II**. All bond lengths and angles in the complexes are within the expected ranges.[33] The order of bond distances to the Ni1 centers is Ni–O < Ni–N < Ni–S < Ni–P, and these distances are comparable to those reported for other nickel(II) complexes containing an O, N and S tridentate thiosemicarbazone and a triphenylphosphine as ligands.[34–36]

Electrochemical studies

The redox properties of the ligands and nickel complexes were studied using CV and SWV measurements in DMSO containing TBAP as the supporting electrolyte on a Pt electrode (Fig. 3 and 4). Table 3 lists the assignments of the redox couples and the electrochemical parameters, which include the half-wave peak potentials ($E_{1/2}$), peak potential separation (ΔE_p), and ratio of

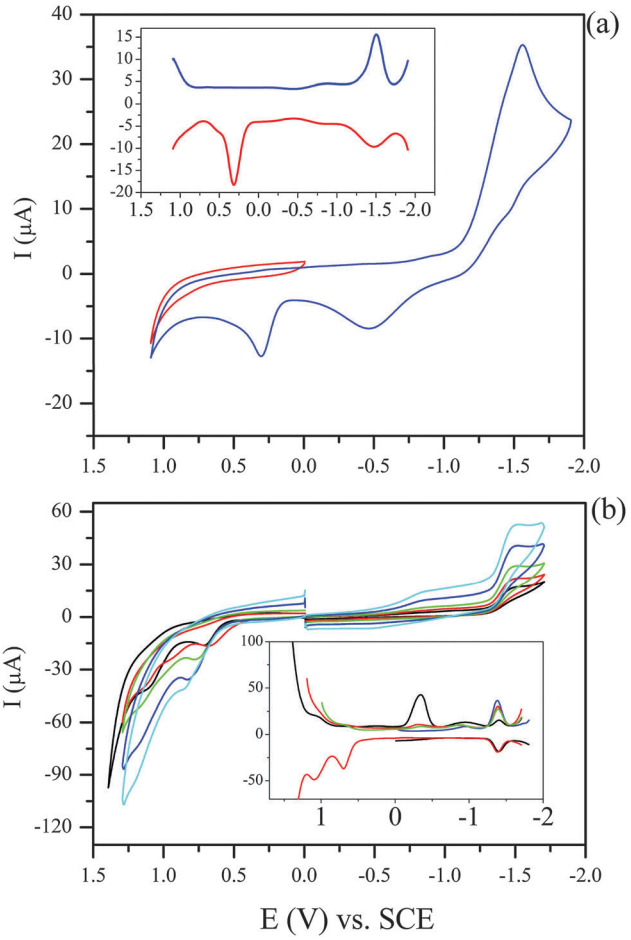

Fig. 3 (a) CV various scan rates of the ligand L_1 (inset: SWV of the ligand L_{II}), (b) CVs of the complex **I** at various scan rates in TBAP/DCM electrolyte system on the Pt working electrode (inset: SWV of the complex **I** recorded with the SWV parameters: pulse size = 100 mV; pulse width = 5 mV; Frequency: 25 Hz).

the reverse scan in order to forward the scan peak currents ($I_{p,rev}/I_{p,for}$). The $E_{1/2}$ values were in conformity with the reported data for redox processes in similar O–N–S complexes.[37–45]

The CV and SWV measurements show that ligands L_1 and L_{II} undergo a one-electron irreversible reduction and/or a one-electron irreversible oxidation processes at the end of the electrolyte windows. The number of transferred electrons was also determined by controlled potential coulometry (CPC) analysis. Similar N_2O_2 type ligands generally give one-electron irreversible reduction processes.[37–45] It was observed that L_1 is reduced and oxidized more easily than L_{II} (Fig. 3 and 4). Although the irreversible reduction process of these ligands was reported for similar ligands,[43–45] oxidation processes of the ligands are rarely reported.[45] Owing to the chemical reactions succeeding the reduction redox processes, the CVs of L_1 show a wave at around −0.30 V, assigned to the chemical reaction products during the reverse potential scans (Fig. 3a). Similarly two waves assigned to the chemical reaction products were recorded at −0.48 and 0.68 V for L_{II} (Fig. 4a). Generally, altering the "R" groups affects the ease of the electron transfer reactions and stability of the electrogenerated species. With respect

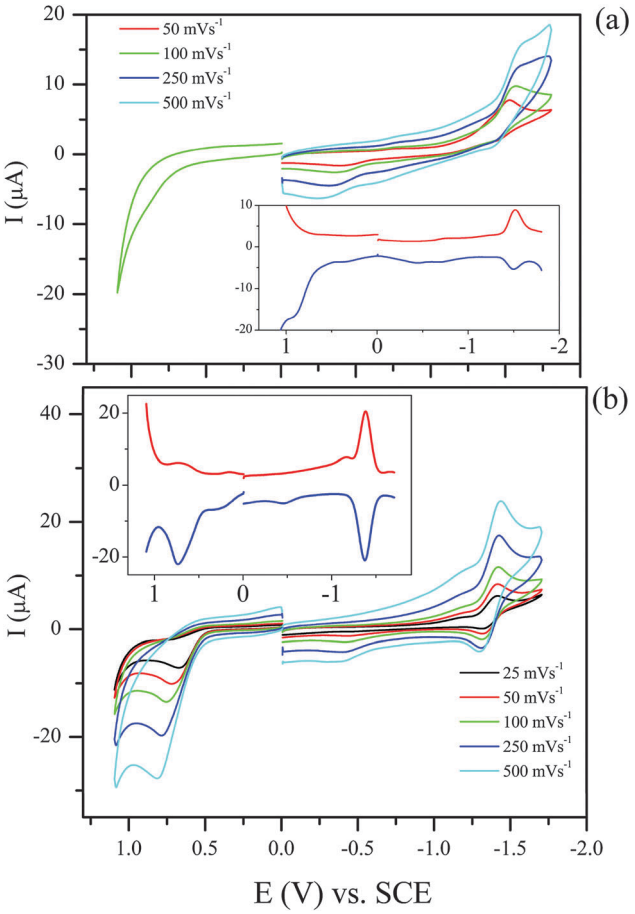

Fig. 4 (a) CV at a 0.100 V s^{-1} scan rate of the ligand $\mathbf{L_{II}}$ (inset: SWV of the ligand $\mathbf{L_{II}}$) in TBAP/DCM electrolyte system on a Pt working electrode (b) CVs of the complex **II** at various scan rates in TBAP/DCM electrolyte system on a Pt working electrode (inset: SWV of the complex **II** recorded the SWV parameters: pulse size = 100 mV; pulse width = 5 mV; Frequency: 25 Hz).

Table 3 Voltammetric data of the compounds

Complex		Ligand oxd.	Metal oxd.	Ligand red.
$\mathbf{L_I}$	$E_{1/2}$ *vs.* SCE[a]	0.90	—	−152
	ΔE_p (mV)[b]	—	—	110
	$I_{p,rev}/I_{p,for}$	—	—	0.40
I	$E_{1/2}$[a]	—	0.73	−1.38
	ΔE_p (mV)[b]	—	200	90
	$I_{p,rev}/I_{p,for}$	—	0.42	0.95
$\mathbf{L_{II}}$	$E_{1/2}$ (V)[a]	1.16	—	−1.63
	ΔE_p (mV)[b]	—	—	—
	$I_{p,rev}/I_{p,for}$	—	—	—
II	$E_{1/2}$[a]	1.09	0.70	−1.51
	ΔE_p (mV)[b]	—	—	105
	$I_{p,rev}/I_{p,for}$	—	—	0.32

[a] $E_{1/2} = (E_{pa} + E_{pc})/2$ at 0.100 V s^{-1}. [b] $\Delta E_p = E_{pa} - E_{pc}$ at 0.100 V s^{-1}.

to the CV and SWV measurements, it can be easily concluded that while methyl carrying a $\mathbf{L_I}$ ligand undergoes electron transfer reaction more easily than an allyl carrying $\mathbf{L_{II}}$ ligand, the electrogenerated species of $\mathbf{L_{II}}$ ligand are chemically more stable than those of the $\mathbf{L_I}$ ligand.

Coordination of the ligands to Ni^{II} ion affects the redox potential of both ligands and metal ion considerably. Especially, the reduction processes of the ligands shifted to positive potentials when coordinated to the electron acceptor Ni^{II} metal ion (Fig. 3b and 4b). It was reported that Ni^{II} complexes undergo a metal-based Ni^{II}/Ni^{I} reduction, or a metal-based Ni^{II}/Ni^{III} oxidation or both of these metal based electron transfer processes depending on the ligand of the complexes.[46–48] For example, the Ni^{II} complex of the dianionic ligand Ni_2bqb^{2-}, [bqb^{2-} = 1,2-bis(quinoline-2-carboxamide)-4,5-dimethyl-benzene dianion], undergoes a reversible Ni^{II}/Ni^{III} oxidation couple at 0.78 V *versus* $Fc^{+/0}$.[49] In another study, Taş and coworkers reported the electrochemical properties of M(II) metal complexes containing *N*,*N*′-(3,4-diaminobenzophenon)-3,5-Bu^t 2-salicylaldimine ligand.[47] In this study, the Ni(II) metal complex indicated a redox couple at 1.32 V *versus* Ag/AgCl assigned to Ni^{II}/Ni^{III}. Hamacher *et al.*[48] reported Ni^{II}/Ni^{I} reduction process for terpyridine nickel complexes and Taner *et al.*[49] reported this reduction process for Ni^{II} calix[4]pyrrole functionalized vic-dioxime complexes.

In this study, Ni complexes, **II** and **I**, undergo a metal-based Ni^{II}/Ni^{III} one-electron irreversible oxidation process at 0.70 V and at 0.73 V, respectively, in addition to the ligand-based redox processes in the TBAP/DMSO electrolyte system (Fig. 3b and 4b). The free ligands do not exhibit a redox process in the potential range where Ni^{2+} oxidation is observed. It was reported that reversibility of the electron transfer processes of Ni complexes also depends on the coordinating ligands.[46–49] The metal-based Ni^{II}/Ni^{III} oxidation processes of **I** and **II** are chemically and electrochemically irreversible with respect to the very large ΔE_p values and very small $I_{p,rev}/I_{p,for}$ ratios. Both **I** and **II** complexes undergo quasi reversible ligand based reduction processes. The ΔE_p values of 90 and 110 mV at 0.100 V s^{-1} scan rate indicate the electrochemically quasi reversible character of the reduction processes of **I** and **II** complexes, respectively. Although these processes are electrochemically quasi reversible, they are chemically irreversible with respect to the small $I_{p,rev}/I_{p,for}$ ratios at all scan rates. When we compared Fig. 3b with Fig. 4a we found that using allyl R groups on the ligand of complexes increases the reversibility of the reduction processes. Thus, redox processes of the complexes carrying allyl group (**II**, Ni$\mathbf{L_{II}}$) are more reversible than those of complex **I**.

Spectroelectrochemical studies

In situ spectroelectrochemical studies were conducted to determine the spectra of the electrogenerated species of the complexes and to assign the redox processes in the CVs of the complexes. Fig. 5 shows *in situ* UV-vis spectral changes in complex **I** in the TBAP/DMSO electrolyte as a representative of the complexes during the controlled potential reductions and oxidation processes. Before any potential application, the complex showed intraligand transition bands at 277 and 316 nm and charge transfer bands at 382 and 440 nm. Under an applied potential at −1.60 V, while the intraligand transition bands at 277 and 316 nm decreased in intensity, the intensity of the charge

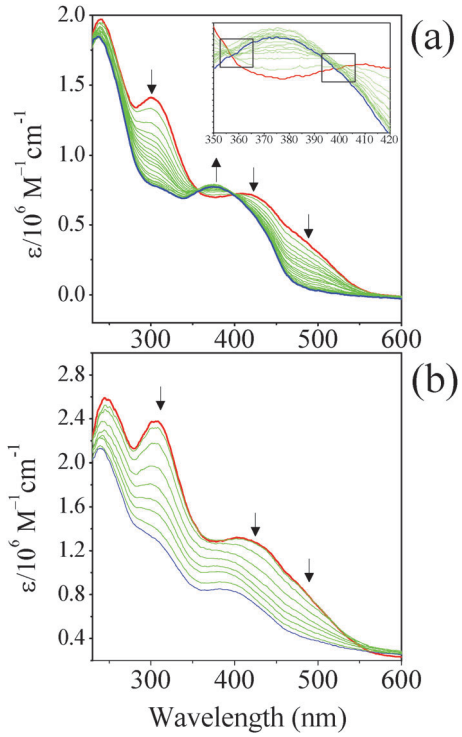

Fig. 5 *In situ* UV-vis spectral changes of **I**. (a) E_{app} = −1.30 V (inset: expanded graph is given to indicate isosbestic points clearly). (b) E_{app} = 0.80 V.

transfer bands at 382 and 440 nm increased (Fig. 5a). These spectroscopic changes indicated a ring-based redox process. The isosbestic point at 365 nm changed with time (inset in Fig. 5a), which demonstrates that the reduction proceeds to give more than a single reduced species, reduced species and the products of a chemical reaction under applied potential at −1.60 V, because the reduction of the complex is followed by successive chemical reactions. The isosbestic points are shown in Fig. 5. We have also expanded the isosbestic point for the clearly recognized isosbestic points observed at nm vibration instead of giving a well-resolved point. This behavior most probably resulted from the chemical irreversibility of the reduction processes. During the potential application of 0.80 V, all bands decreased in intensity and any clear isosbestic point was recorded at the beginning of the oxidation process. After a while, the band at 316 nm started to increase in intensity while the other band decreased (Fig. 5b). These spectroscopic changes are characteristic of the decomposition of the complex during oxidation.

Conclusion

The synthesis and characterization of 5-chloro-2-hydroxybenzophenone-*N*-methyl thiosemicarbazone ($\mathbf{L_I}$) and 5-chlorobenzophenone-*N*-allyl thiosemicarbazone ($\mathbf{L_{II}}$) and their Ni(II) complexes (**I**, **II**) with triphenylphosphine was achieved by physicochemical, spectroscopic methods and single-crystal X-ray diffraction. The IR, UV, ^{1}H- and ^{31}P-NMR spectral studies lead to the conclusion that the thiosemicarbazone behave as a tridentate ligand coordinated to a nickel(II) atom through azomethine nitrogen, thiol sulphur and phenolic oxygen atoms. The lone pairs on the phosphor atom of triphenylphosphine molecule as a second ligand are used to form a fourth bond with an empty orbital in the nickel(II) ion. Complexes, **I** and **II**, crystallize in the monoclinic space group $P2_1/a$ with four molecules in the unit cell. It was found that the complexes have a distorted square planar geometry. The electrochemical results show that the ligands undergo a one-electron irreversible reduction and/or a one-electron irreversible oxidation process at the end of the electrolyte windows with CV and SWV measurements. It was observed that thiosemicarbazone ligands can undergo oxidation and $\mathbf{L_I}$ is reduced and oxidized more easily than $\mathbf{L_{II}}$ in this study. Ni complexes, **II** and **I**, undergo a metal-based Ni^{II}/Ni^{III} one-electron irreversible oxidation process in addition to the ligand-based redox processes in the TBAP/DMSO electrolyte system. The metal-based Ni^{II}/Ni^{III} oxidation processes of **II** and **I** are chemically and electrochemically irreversible.

Acknowledgements

This work was supported by the Scientific Research Projects Coordination Unit of Istanbul University (Project Numbers: BAP 16682 and UDP-26770).

Notes and references

1 C.-P. Wu, S. Shukla, A. Maria Calcagno, M. D. Hall, M. M. Gottesman and S. V. Ambudkar, *Mol. Cancer Ther.*, 2007, **6**, 3287.
2 Z. G. Jiang, M. S. Lebowitz and H. A. Ghanbari, *CNS Drug Rev.*, 2006, **12**(1), 77.
3 J. A. Ludwig, G. Szakács, S. E. Martin, B. F. Chu, C. Cardarelli, Z. E. Sauna, N. J. Caplen, H. M. Fales, S. V. Ambudkar, J. N. Weinstein and M. M. Gottesman, *Cancer Res.*, 2006, **66**, 4808.
4 G. Atassi, P. Dumont and J. C. Harteel, *Eur. J. Cancer*, 1979, **15**, 451.
5 B. Atasever, B. Ülküseven, T. Bal-Demirci, S. Erdem-Kuruca and Z. Solakoğlu, *Invest. New Drugs*, 2010, **28**, 421.
6 R. Yanardag, T. Bal Demirci, B. Ülküseven, S. Bolkent, S. Tunalı and Ş. Bolkent, *Eur. J. Med. Chem.*, 2009, **44**, 818.
7 A. E. Liberta and D. X. West, *BioMetals*, 1992, **5**(2), 121.
8 H. Ali Zamani, *Anal. Lett.*, 2008, **41**(10), 1850.
9 M. Arab Chamjangali, S. Soltanpanah and N. Goudarzi, *Sens. Actuators, B*, 2009, **138**(1), 251.
10 W. Lu, H. Jiang, F. Hu, L. Jiang and Z. Shen, *Tetrahedron*, 2011, **67**, 7909.
11 Nuriman, B. Kuswandi and W. Verboom, *Sens. Actuators, B*, 2011, **157**(2), 438.
12 (*a*) G. Reinert, *Process for photochemical stabilization of polyamide fiber material and mixtures thereof with other fibers: water-soluble copper complex dye and light-stabilizer*, *US Pat.*, 4,874,391, Ciba-Geigy Corporation, 1989; (*b*) T. N. Myers, *2-Hydroxybenzophenone Hydrazides and Derivatives Thereof*, *US Pat.*, 5,041,545, Atochem North America, Inc., 1991; (*c*) K. Nobuo, T. Masataka and T. Takashi,

Polarizing plate and liquid crystal display device, Patent (US 20110058129, WO 2009139284 A1, KR 20110002085 A), Konica Minolta Opto Inc., 19 Nov 2009–10 Mar 2011; (*d*) R. Yamada and A. Matsuda, *Optical Film, Polarizing Plate And Display Device Using The Same, And Manufacturing Method Thereof*, *US Pat.*, 8,158,218 B2, Konica Minolta Opto, Inc., 2012.

13 K. B. Chakraborty and G. Scott, *Eur. Polym. J.*, 1979, **15**(1), 35.
14 Y. Dobashi, J.-I. Kondou and Y. Ohkatsu, *Polym. Degrad. Stab.*, 2005, **89**, 140.
15 K. Bentayeb, L. K. Ackerman, T. Lord and T. H. Begley, *Food Addit. Contam., Part A*, 2013, **30**(4), 750.
16 M. Placzek, M. Dendorfer, B. Przybilla, K. P. Gilbertz and B. Eberlein, *Acta Derm.-Venereol.*, 2013, **93**(1), 30.
17 R. Prabhakaran, R. Sivasamy, J. Angayarkanni, R. Huang, P. Kalaivani, R. Karvembu, F. Dallemer and K. Natarajan, *Inorg. Chim. Acta*, 2011, **374**, 647.
18 S. I. Mostafa, A. A. El-Asmy and M. S. El-Shahawi, *Transition Met. Chem.*, 2000, **25**, 470.
19 B. İlhan Ceylan, Y. Daşdemir Kurt and B. Ülküseven, *J. Coord. Chem.*, 2009, **62**(5), 757.
20 G. E. Chavarria, M. R. Horsman, W. M. Arispe, G. D. Kishore Kumar, S.-E. Chen, T. E. Strecker, E. N. Parker, D. J. Chaplin, K. G. Pinney and M. Lynn Trawick, *Eur. J. Med. Chem.*, 2012, **58**, 568.
21 T. S. Lobana, P. Kumari, R. J. Butcher, T. Akitsu, Y. Aritake, J. Perles, F. J. Fernandez and M. C. Vega, *J. Organomet. Chem.*, 2012, **701**(15), 17.
22 A. Arquero, M. Antonia Mendiola, P. Souza and M. Teresa Sevilla, *Polyhedron*, 1996, **15**(10), 1657.
23 R. M. El-Shazly, G. A. A. Al-Hazmi, S. E. Ghazy, M. S. El-Shahawi and A. A. El-Asmy, *Spectrochim. Acta, Part A*, 2005, **61**, 243.
24 *Rigaku, PROCESS-AUTO*, Rigaku Corporation, Tokyo, Japan, 1998.
25 *Rigaku/MSC, CRYSTALSTRUCTURE Version 3.5.1*, Rigaku/MSC, The Woodlands, Texas, USA, 2003.
26 G. M. Sheldrick, *Acta Crystallogr., Sect. A: Found. Crystallogr.*, 2008, **64**, 112.
27 L. J. Farrugia, *J. Appl. Crystallogr.*, 2012, **45**, 849.
28 L. J. Farrugia, *J. Appl. Chem.*, 1997, **30**, 565.
29 Ş. Güveli, T. Bal Demirci, N. Özdemir and B. Ülküseven, *Transition Met. Chem.*, 2009, **34**, 383.
30 B. Ulkuseven, T. Bal-Demirci, M. Akkurt, Ş. Pınar Yalçın and O. Buyukgungor, *Polyhedron*, 2008, **27**, 3646.
31 E. Ramachandran, P. Kalaivani, R. Prabhakaran, N. P. Rath, S. Brinda, P. Poornima, V. V. Padma and K. Natarajan, *Metallomics*, 2012, **4**, 218.
32 A. B. P. Lever, *Inorganic Electronic Spectroscopy*, Elsevier, Amsteredam, 1984.
33 F. H. Allen, O. Kennard, D. G. Watson, L. Brammer, A. G. Orpen and R. Taylor, *J. Chem. Soc., Perkin Trans. 2*, 1987, **12**, 11.
34 R. Prabhakaran, R. Karvembu, T. Hashimoto, K. Shimizu and K. Natarajan, *Inorg. Chim. Acta*, 2005, **358**, 2093.
35 P. X. García-Reynaldos, S. Hernández-Ortega, R. A. Toscano and J. Valdés-Martínez, *Supramol. Chem.*, 2007, **A19**, 613.
36 Ş. Güveli, N. Özdemir, T. Bal-Demirci, B. Ülküseven, M. Dinçer and Ö. Andaç, *Polyhedron*, 2010, **29**, 2393.
37 M. Kandaz, İ. Yılmaz, S. Keskin and A. Koca, *Polyhedron*, 2002, **21**, 825.
38 M. Kandaz, A. Koca and A. R. Özkaya, *Polyhedron*, 2004, **23**, 1987.
39 M. Kato, K. Nakajima, Y. Yoshikawa, M. Hirotsu and M. Kojima, *Inorg. Chim. Acta*, 2000, **311**, 69.
40 P. Barbaro, C. Bianchini, G. Scapacci, D. Masi and P. Zanello, *Inorg. Chem.*, 1994, **33**, 3180.
41 A. P. Rebolledo, O. E. Piro, E. E. Castellano, L. R. Teixeira, A. A. Batista and H. Beraldo, *J. Mol. Struct.*, 2006, **794**, 18.
42 M. El-Shazly, G. A. A. Al-Hazmi, S. E. Ghazya, M. S. El-Shahawi and A. A. El-Asmya, *Spectrochim. Acta, Part A*, 2005, **61**, 243.
43 A. I. Matesanz, J. Mosa, I. Garćia, C. Pastor and P. Souza, *Inorg. Chem. Commun.*, 2004, **7**, 756.
44 A. Arquero, M. A. Mendiola, P. Souza and M. T. Sevilla, *Polyhedron*, 1996, **15**, 1657.
45 D. Mishra, S. Naskar, M. G. B. Drew and S. K. Chattopadhyay, *Inorg. Chim. Acta*, 2006, **359**, 585.
46 S. Meghdadi, K. Mereiter, A. Amiri, N. S. Mohammadi, F. Zamani and M. Amirnasr, *Polyhedron*, 2010, **29**, 2225.
47 E. Taş, A. Kilic, M. Durgun, L. Küpecib, I. Yilmaz and S. Arslan, *Spectrochim. Acta, Part A*, 2010, **75**, 811.
48 C. Hamacher, N. Hurkes, A. Kaiser, A. Klein and A. Schüren, *Inorg. Chem.*, 2009, **48**, 9947.
49 B. Taner, P. Deveci, S. Bereket, A. Osman Solak and E. Özcan, *Inorg. Chim. Acta*, 2010, **363**, 4017.